ACS Sustainable Chemistry & Engineering

Research Article

pubs.acs.org/journal/ascecg

Facile Synthesis of Fe_3O_4@g-C Nanorods for Reversible Adsorption of Molecules and Absorption of Ions

Daniel Suma[†] and Da Deng*[,‡]

[†]Department of Chemcial and Biomolecular Engineering, University of Notre Dame, Notre Dame, Indiana 46556, United States

[‡]Department of Chemical Engineering and Materials Science, Wayne State University, Detroit, Michigan 48202, United States

Supporting Information

ABSTRACT: It is an interesting but challenging task to design a facile and scalable procedure for the making of multifunctional materials for energy and environmental applications. Here, we developed a one-pot facile procedure for the preparation of disordered carbon (a-C) coated Fe_2O_3 nanorods. By heating Fe_2O_3@a-C nanorods under argon, they were easily converted to graphite carbon (g-C) coated magnetic Fe_3O_4, or Fe_3O_4@g-C, nanorods. We demonstrated that the as-prepared magnetic Fe_3O_4@g-C nanorods could reversibly store molecules, using dye as a model. This suggested that one of the possible applications would be as recyclable and reusable adsorbents for water remediation. At the same time, the magnetic Fe_3O_4@g-C nanorods are proposed as vehicles for the controlled release of drugs in an aqueous environment and, in particular, for the targeted treatment of infected regions through guided external magnetic forces. The Fe_3O_4@g-C nanorods were also investigated for their performances in the reversible storage of sodium ions, which is closely relevant to future sodium-ion batteries. We discovered that thin graphite carbon sheaths, which encapsulate the high-capacity Fe_3O_4 cores, could actually prevent the cores from having full access to sodium ions. We suggested that carbon coating, commonly used in electrode materials for lithium-ion batteries, may not be generally suitable for electrode materials used in future sodium-ion batteries. This discovery is helpful in guiding future studies on the use and selection of carbon coating, a common strategy to overcome electrode pulverization in lithium-ion batteries, for electrodes in future sodium-ion batteries.

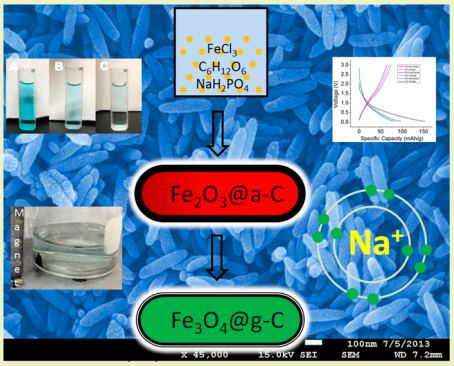

KEYWORDS: *One-pot, hydrothermal, core−shell, adsorption, desorption, sodium-ion battery*

INTRODUCTION

The pressing issues of environmental pollution and the depletion of nonrenewable energy resources require that innovative technologies be developed. The industrialized society generates a significant amount of toxic chemicals that could enter and pollute our environment. For example, nonbiodegradable dyes are used in textile, paper, and residential industries, and can pose severe threats to aqueous environments. Therefore, the elimination of harmful chemicals, including dyes, from wastewater is one of the challenging goals for environmental engineers. On the other hand, renewable energy from solar and wind sources will help to reduce our dependence on nonrenewable fossil fuels and develop a sustainable society. The intermittent energy will require reliable low-cost rechargeable batteries that will be integrated into the smart grids of the future. Lithium-ion batteries are too expensive to be used in future smart grids. Therefore, the development of alternative low-cost rechargeable batteries, such as sodium-ion batteries, could potentially change the market of rechargeable batteries.

Functional materials that address the issues mentioned above have recently attracted much attention. For example, TiO_2 nanoparticles are being used as photocatalysts in order to decompose organic contaminants;[1,2] carbon nanoparticles, including nanotubes, are being used to adsorb toxic compounds in wastewater;[3] and silver nanoparticles are employed to disinfect water.[4] There are actually quite a few widely investigated functional nanomaterials that have been proposed for the removal of pollutants from wastewater.[5] However, one of the main issues in using conventional nanoparticles to treat wastewater is that it is very difficult to reuse or even remove the nanoparticles after applications. In certain cases, the nanoparticles could turn out to be secondary pollutants themselves. Nontoxic nanoparticles with strong magnetic properties that can easily be removed after use and recycled are better candidates than conventional nanoparticles. Fe_3O_4 is nontoxic and can be easily collected by external magnetic forces, at least in static state in laboratories. When Fe_3O_4 is further encapsulated in carbon, the magnetic Fe_3O_4 core is protected from attacks by dissolved aqueous species. In terms of functional materials for energy storage in sodium-ion batteries, a number of materials have been explored.[6−10] For example, nanoparticles of $NaVPO_4F$,[11] $Na_{0.44}MnO_2$,[12] $Na_xCo[Fe(CN)_6]_{0.90}\cdot 2.9H_2O$,[13] layered $Na_{0.71}CoO_2$,[14] $KFe_{(II)}Fe_{(III)}(CN)_6$,[15] and Na_2FePO_4F,[16] have been explored for positive electrode materials. Negative

Received: October 3, 2014
Revised: November 23, 2014
Published: December 3, 2014

electrode materials have been relatively less explored. Fe_3O_4 recently demonstrated good electrochemical performance in reversible ion storage.[17−21] However, these materials have poor cyclability due to electrode pulverization and poor conductivity. Carbon coated Fe_3O_4 nanoparticles are generally accepted, in the community of lithium-ion batteries, to overcome those issues. However, it is still an open question whether carbon coating is also beneficial in the case of sodium-ion batteries.

Herein, we report a facile one-step hydrothermal preparation of Fe_2O_3@a-C nanorods which can easily be converted to Fe_3O_4@g-C nanorods by heating in an inert gas. We investigated the performances of the as prepared Fe_3O_4@g-C nanorods in reversibly adsorbing/releasing molecules, using a dye as the model, in water. We also investigated the reversible storage of ions, namely, electrochemical insertion/extraction of sodium ions, which is closely relevant to sodium-ion batteries. The experimental evidence clearly revealed the advantages and disadvantages of the Fe_3O_4@g-C nanorods in those applications. It is particularly interesting to highlight that we discovered that carbon coating, although popularly employed in lithium-ion batteries, may actually not be good for sodium-ion batteries.

EXPERIMENTAL SECTION

Materials Preparation. All chemicals were used as received. The precursor Fe_2O_3@a-C nanorods were prepared by a one-step hydrothermal method modified from a method for the preparation of bare Fe_2O_3 nanospindles.[22] Typically, 2.2 mg of $NaH_2PO_4{\cdot}H_2O$ and 2.8 mg of D-glucose were dissolved in 35 mL of water under stirring for 10 min, followed by the addition of 151.2 mg of $FeCl_3{\cdot}6H_2O$ and stirred for an additional 10 min. The solution was then transferred into an autoclave and heated to 180 °C and held for 24 h. The products were thoroughly washed by water and ethanol and dried in a vacuum oven at 50 °C overnight. The Fe_3O_4@g-C nanorodes were derived from the precursor Fe_2O_3@a-C nanorods. The precursor in powder form was placed in a crucible boat loosely covered and inserted into a tube furnace. The tube furnace was purged by argon for 1 hour to eliminate air. The furnace was heated up at a ramp rate of 6 °C/min to 600 °C and maintained at 600 °C for 2 h under an argon flow rate of 100 SCCM and then naturally cooled down with the same gas to room temperature. The overall conversion is illustrated in Figure 1.

Materials Characterization. Powder X-ray diffraction (XRD) was carried out with Rigaku Smartlab X-ray diffractometer using Cu Kα radiation (λ = 0.154 18 nm). The morphologies of the products were characterized by field emission scanning electron microscopy (JSM-7600 FE SEM) and transmission electron microscopy (JEOL 2010 TEM instrument, with an accelerating voltage of 200 kV).

Reversible Adsorption of Molecules. For the reversible molecular adsorption trial, a solution of 2 mg/L methylene blue was used to mimic organic polluted water. Typically, 5 mg of the Fe_3O_4@g-C nanorods was dispersed in 12 mL of the dyed water under stirring on a magnetic stirrer. (Note: no stirring bar was used; instead the innate magnetic properties of the Fe_3O_4@g-C nanorods allowed them to self stir.) The concentration change was monitored at different time intervals by a Shimadzu UV-2600 spectrophotometer using the absorbance peak of methylene blue at 664 nm. Every 10 min, 3 mL of liquid was taken out, put in a cuvette, and measured by a UV spectrometer. After measurement, the 3 mL solution was returned to the mother solution. After the purification process, these Fe_3O_4@g-C nanorods were collected by a magnet that could be backwashed and used again.

For the desorption trial, which could simulate drug delivery, the Fe_3O_4@g-C nanorods were saturated with adsorbed methylene blue by exposing them to a methylene blue solution (12 mg/L) for 4 h and then collected by a magnet. They were then placed in 12 mL of water and stirred using a magnetic stirrer without the stirring bar as before. The beaker was covered with parafilm and wrapped with aluminum foil to prevent evaporation and light-induced decomposition. The concentration or the amount of dye released was determined similarly by a UV spectrometer.

Reversible Absorption of Ions. A homogeneous slurry was prepared by thoroughly mixing the as-synthesized Fe_3O_4@g-C nanorods as active materials and polyvinylidene fluoride (PVDF) as a binder in a weight ratio of 90:10 in *N*-methylpyrrolidone (NMP). It should be highlighted that no carbon black was added as conductive enhancer, in contrast to typical electrode preparation. The slurry was applied to a copper disc current collector and dried in a vacuum oven at 100 °C for 24 h. Electrochemical test cells were assembled in an argon-filled glovebox using the coated copper disc as the working electrode, metallic sodium as the counter and reference electrode, and 1 M $NaClO_4$ in ethylene carbonate (EC):propylene carbonate (PC) (1:1 in volume) was used as the electrolyte and PP/PE/PP trilayer membranes (Celgard 2320) as the separator. The testing cells were charged and discharged galvanostatically at room temperature in the voltage window of 0.04−3 V at different current rates to evaluate their properties in the reversible storage of sodium ions.

RESULTS AND DISCUSSION

The chemical compositions of one-pot prepared Fe_2O_3@a-C and the derived Fe_3O_4@g-C nanorods were characterized by XRD (Figure 2). The one-pot hydrothermally obtained Fe_2O_3@a-C

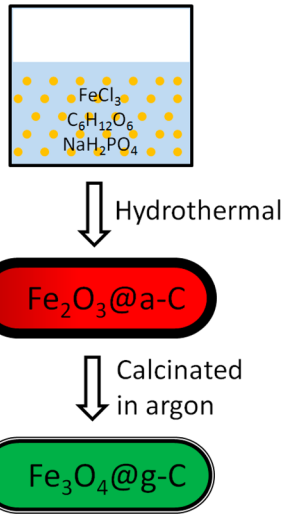

Figure 1. Schematic showing the one-step formation of Fe_2O_3@a-C nanorods and subsequent conversion to Fe_3O_4@g-C nanorods by calcination in argon.

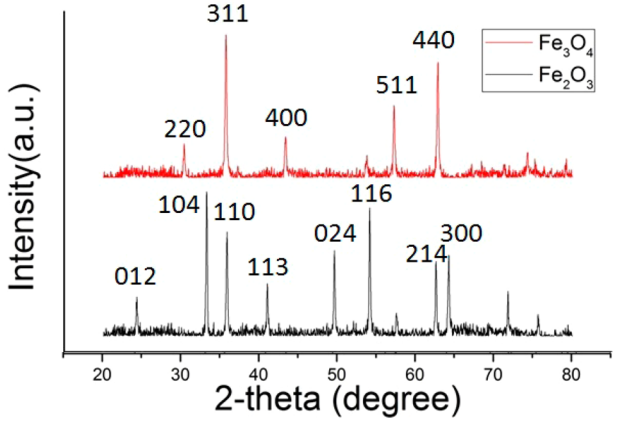

Figure 2. XRD patterns of (a) Fe_2O_3@a-C nanorods and (b) Fe_3O_4@g-C nanorods after calcination.

dx.doi.org/10.1021/sc500629p | ACS Sustainable Chem. Eng. 2015, 3, 133−139

nanorods demonstrated clear diffraction peaks which could be assigned to α-Fe_2O_3 (JCPDS card #89-8013). No peaks associated with carbon could be distinguished suggesting that the carbon sheaths derived from the carbonization of glucose are mainly amorphous.[23] The carbonization of glucose under hydrothermal conditions above 160 °C forming amorphous carbon is well documented.[23−27] After calcination at 600 °C in argon, the Fe_2O_3@a-C nanorods were completely converted toFe_3O_4@g-C nanorods, as evidenced by XRD (Figure 2). All the XRD peaks can be assigned to Fe_3O_4 (JCPDS Card No.75-0449), while no Fe_2O_3 peaks from its precursor can be distinguished. This indicates that carbothermic conversion of Fe_2O_3 into Fe_3O_4 was successful and complete. The calcinated powder of Fe_3O_4@g-C nanorods can be attracted by a magnet, also demonstrating that Fe_2O_3, which is antiferromagnetic, was successfully converted to Fe_3O_4, which is ferromagnetic. The conversion from Fe_2O_3 to Fe_3O_4 under inert gas also proves the existence of carbon sheaths that were produced by the hydrothermal carbonization of glucose. These carbon sheaths act as the reducing agent that partially transforms Fe_2O_3 to Fe_3O_4. Again, no visible carbon peaks suggests that the carbon sheaths are too thin (as revealed by TEM) to be detected.[28,29]

The structure of the one-pot synthesized Fe_2O_3@a-C nanorods were thoroughly characterized by field emission scanning electron microscopy (FESEM) and transmission electron microscopy (TEM) micrographs (Figure 3). The low-magnification FESEM image suggests a large amount of nanorodes with good size distribution were synthesized by the hydrothermal method (Figure 3a). The nanorods are about 200 nm in length and 70 nm in diameter (Figure 3b). We noticed that it was difficult to focus on the nanorods under SEM in order to take sharp images. This observation suggests that the carbon coated on the surface of nanorods has poor conductivity, as expected. The poor conductivity of the carbon derived from the carbonization of glucose is due to a low degree of graphitization and presence of functional groups. The carbon sheaths encapsulating Fe_2O_3 nanorods were more clearly visible from TEM images (Figure 3c,d). The light contrast surrounding the dark core of each nanorod suggests that the carbon sheaths could encapsulate and cover the whole nanorod. The carbon sheath is about 5−10 nm in thickness and is distributed continuously on the surface of each nanorod (Figure 3c). Experimentally, it was observed that the carbon coating is continuous, but not uniformly thick around the Fe_2O_3 nanorods (Figure S2e in the Supporting Information). The effects of various experimental conditions on the morphology of the products were investigated. When less amount of $FeCl_3$ (e.g., 38 mg instead of 151 mg typically used) was used, keeping other experimental parameters unchanged, no nanorods could be formed (Figure S2a,b in the Supporting Information). In another case, we tried to increase the reaction time from 24 to 48 h, and the as-obtained nanorods had smaller aspect ratios (Figure S2c-d in the Supporting Information) as compared to those obtained after 24 h of reaction (Figure 3). Additionally, we tried to add in CTAB as a stabilizer/surfactant to reveal its influence on morphology control, again no nanorods could be obtained with the presence of CTAB regardless of reaction time (Figure S3 in the Supporting Information). In other words, the morphology and carbon coating are very much depended on the experimental conditions.

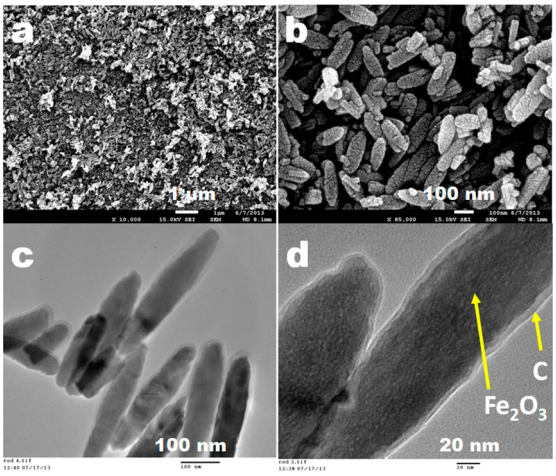

Figure 3. One-pot synthesized Fe_2O_3@a-C nanorods: FESEM images of (a) low-magnification overall view and (b) zoom-in view; TEM images of (c) low-magnification view of a few representative nanorods with light contrast of carbon coating the surface visible and (d) high-magnification view of a section of two nanorods shows the carbon sheath and Fe_2O_3 core more clearly.

Fe_3O_4@g-C nanorods were simply derived from Fe_2O_3@a-C nanorods by calcination in an inert gas based on carbothermic reduction. In addition to XRD, the optical color is typically black Fe_3O_4 rather than the usual red color of Fe_2O_3.[30,31] The nanorods could be attracted by a magnetic bar (inset of Figure 4a), which also demonstrated that Fe_2O_3 was successfully converted to Fe_3O_4. The conversion from Fe_2O_3 to Fe_3O_4 under inert gas also proves the existence of carbon sheaths that were derived from the carbonization of glucose under one-pot hydrothermal conditions. Carbon sheaths act as the only reducing agent to reduce Fe_2O_3 to Fe_3O_4. The morphology of the as-derived Fe_3O_4@g-C nanorods was revealed by FESEM and TEM images (Figure 4). After calcination at 600 °C under Ar, the overall morphology was well preserved (Figure 4a,b). We noticed that it was easier to focus on the nanorods under SEM to take sharp images as compared to its precursors before calcination. This observation suggests that the carbon coated

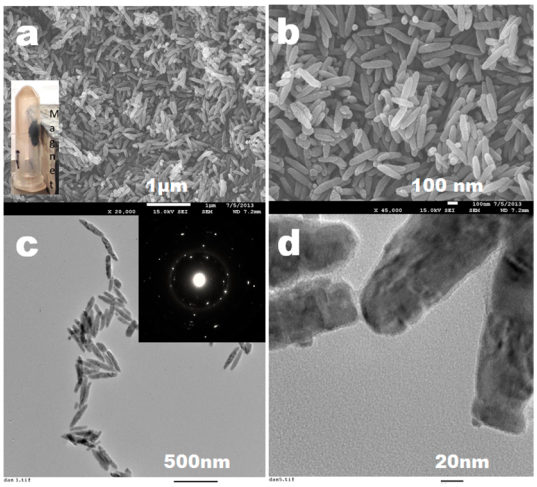

Figure 4. FESEM and TEM images of the derived Fe_3O_4@g-C nanorods: (a, b) SEM images at low-magnification and high-magnification; inset of (a) is the optical image showing the nanorods can be attracted by a magnet; (c, d) TEM images of Fe_3O_4@g-C nanorods at low-magnification and high-magnification respectively; inset of c is the corresponding SAED pattern.

dx.doi.org/10.1021/sc500629p | ACS Sustainable Chem. Eng. 2015, 3, 133−139

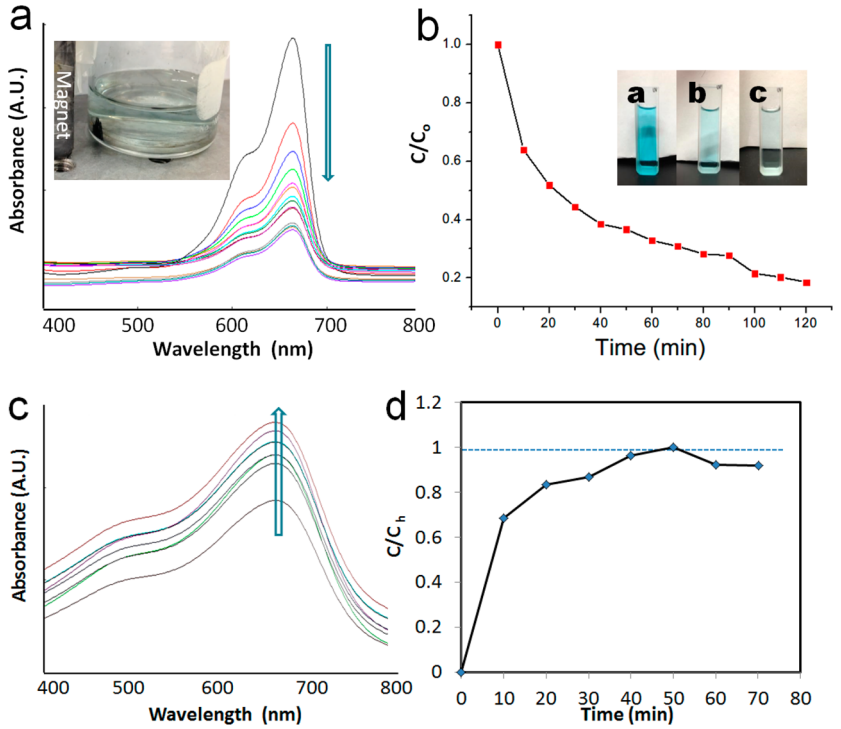

Figure 5. Reversible adsorption magnetic Fe_3O_4@g-C nanorods as recoverable adsorbents: (a) UV−vis spectra of the methylene blue solution with increasing adsorption times; inset of (a) shows a magnet being used to recover the nanorods in a beaker; (b) normalized concentration for increasing adsorption times; inset of b shows the optical images of the decay in color of the solution over time; (c) UV−vis spectra of the methylene blue solution with increasing desorption times; (b) normalized concentration for increasing desorption times.

on the surface of the nanorods has dramatically improved conductivity due to annealing induced enhanced graphitization. In other words, the amorphous carbon sheaths have been converted to graphitic carbon. The selected area electron diffraction (SAED) pattern (inset of Figure 4c) demonstrates that the core Fe_3O_4 nanorods are crystalline and all the diffraction spots can be assigned to Fe_3O_4, agreeing with XRD. The low-magnification TEM image clearly shows that the overall morphology is still the same as the precursor (Figure 4c). The high-magnification TEM image clearly shows that there is still carbon encapsulating each nanorod (Figure 4d). The light contrast surrounding the dark core of each nanorod suggests that the carbon sheaths completely encapsulate all of the nanorods. The carbon sheath is about 3 nm in thickness and is uniformly distributed continuously on the surface of each nanorod. The heat treatment combined with the presence of iron provides the right conditions for the catalytic graphitization of the sheaths into highly graphitic carbon, is well documented.[29,30] The reduced thickness of the carbon sheaths when compared to its precursor is ascribed to the consumption of carbon and graphitization, as expected.

Reversible Adsorption of Molecules. A proof-of-concept demonstration was carried out to use Fe_3O_4@g-C nanorods for the reversible adsorption and desorption of a typical dye in an aqueous environment. In this case, methylene blue was selected as a typical organic pollutant to test the ability of the Fe_3O_4@g-C nanorods for adsorptive removal of organic pollutants from water. Figure 5a is the UV−vis spectra of a methylene blue solution for progressive contact with self-stirring Fe_3O_4@g-C nanorods on a stirrer without a stirring bar. The absorbance decreases continuously over time, indicating that the Fe_3O_4@g-C nanorods can effectively adsorb the dye from the solution. This process described is physical adsorption, as there are no other UV−vis peaks observed or no new chemical components generated. The carbon sheaths can prevent the exposure of the catalytically active Fe_3O_4 to the dye molecules.[32] The magnetic Fe_3O_4 core enables the easy collection of the nanoparticles. This easy collection allows for the avoidance of the nanoparticles themselves becoming an additional pollutant. The inset of Figure 5a shows that the solid/liquid separation is rather easy and that the nanoparticles can be facilely collected by a magnet, at least at static state. The mechanism of dye adsorption should be the same as that of activated carbon and is associated with (1) the electrostatic attraction between the negatively charged surface oxygen-containing groups and cationic methylene blue; (ii) the good contact between the self-stirring, nonaggregate nanorods and dye molecules. Therefore, considering relatively high adsorption capacity, rapid adsorption rate, and convenient magnetic separability of the Fe_3O_4@g-C nanorods, these materials could be a promising alternative adsorbent for the removal of toxic species from water. It is important to note that pure Fe_3O_4 has no ability to adsorb the methylene blue molecule.[33] This means that the excellent absorption ability is a direct result of the carbon sheaths that serve the double roles of protective skins for the Fe_3O_4 cores and functional adsorbents. Figure 5b shows that the normalized concentration of methylene blue in solution decreases with time, with an 80% loss of dye from solution over 2 h.

The surface area of the Fe_3O_4@C nanorods was estimated to be 13.7 m^2/g. The adsorption capacity in our not optimized, preliminary test was estimated to be ~5.8 mg methylene blue/g Fe_3O_4@C nanorods. The adsorption capacity of methylene blue was reported in the range between 100−420 mg methylene blue/g activated carbon derived from bamboo.[34] The initial concentration of methylene blue used in this study was in the range from 100−500 mg/L. The surface area of the activated

dx.doi.org/10.1021/sc500629p | ACS Sustainable Chem. Eng. 2015, 3, 133−139

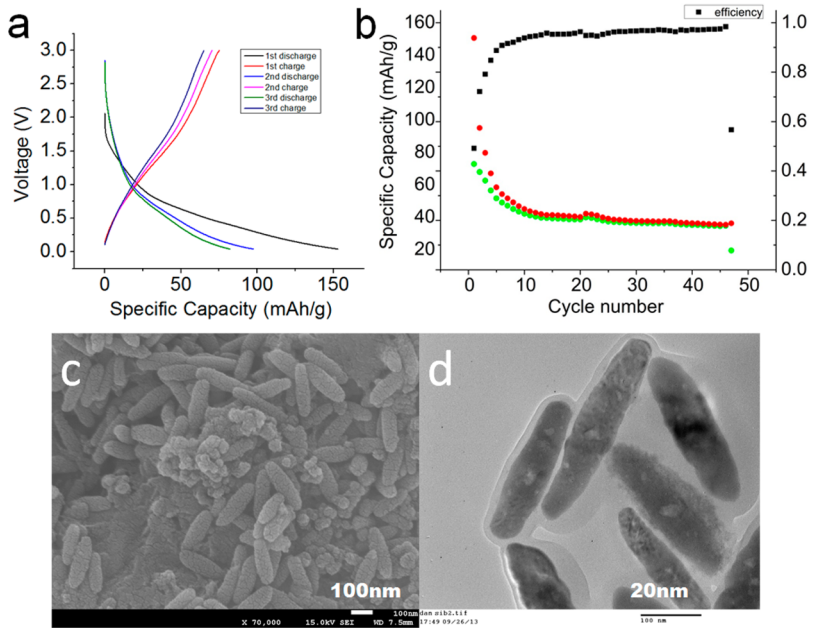

Figure 6. Electrochemical performance of Fe_3O_4@g-C nanorods for reversible storage of sodium ions: (a) first three cycle insertion−extraction profiles; (b) cycling performance in sodium ion storage; morphology retention of Fe_3O_4@g-C nanorods after cycling: (c) FESEM overall view and (d) TEM image showing the well preserved core−shell structure.

carbon derived from bamboo following a complex procedure is about 1896 m^2/g. If one considers the efficiency in utilization of surface area, our Fe_3O_4@C nanorods have an adsorption capacity of 0.42 mg/m^2; in comparison, the activated carbon derived from bamboo has an adsorption capacity of 0.05−0.22 mg/m^2 only. In other words, the surface area of our Fe_3O_4@C nanorods is more efficiently utilized in the adsorption of MB even at a very low concentration of 2 mg/L. These results show that the Fe_3O_4@g-C nanorods can potentially be used as a magnetic adsorbent for the remove of dye contaminants in water. As an additional note, these nanoparticles could conceivably be used in many current disasters that involve the purification of chemicals from water supplies. For example, the recent spill of 4-methylcyclohexanemethanol into the Elk River water supply could have been systematically removed in large quantities so that fresh, clean water could be distributed to the citizens in a timely fashion.

The Fe_3O_4@g-C nanorods also have the impressive, unique capability of desorption of substances. As shown in Figure 5c, it can be clearly seen that these Fe_3O_4@g-C nanorods release the methylene over time. Specifically, in the first 10 min, the 69% (using the baseline of maximum concentration of methylene in the whole process) methylene was released into purer water. After that, a stable release rate was recorded in the span of 60 min. This observation provides evidence that the materials can be used to deliver a medicine or material over time, or keep a concentration steady in a specific solution. This observation implies that the Fe_3O_4@g-C nanorods can be recycled and reused. At the same time, the capability of desorption can mimic controlled delivery processes. In a biological or pharmaceutical arena, the material can be used to deliver compounds or drugs over time. As the compounds are digested by parts of the biological system, or the carrying-particles are moved from place to place, the particles can continue to slowly distribute the medicine. In other words, the magnetic Fe_3O_4@g-C nanorods can be employed as a vehicle for the controlled release of drugs in an aqueous environment as well as be used in the targeted treatment of specific locations through guided external magnetic forces. One may notice that the size of 200 nm could be a bit too large for drug delivery. On the other hand, spherical Fe_3O_4 particles without graphitic carbon coating at size of 200 nm in diameter have been demonstrated to be promising anticancer drug carriers.[35] Therefore, our facilely prepared magnetic particles coated with graphitic carbon with enhanced stability may be worthy of further studies as potential drug delivery carriers.

Reversible Absorption of Ions. Theoretically, magnetite has a high capacity of 926 mAh/g based on the conversion-type mechanism of electrochemical sodium insertion.[36−38] However, Fe_3O_4 suffers massive volume expansion upon electrochemical ion insertion.[39] The so-called pulverization could cause the disintegration of the electrode and lead to poor cycling performance. Additionally, Fe^0 nanograins from electrochemical conversion reactions may be highly reactive toward the organic electrolyte and can decompose electrolytes.[37,38] One popular strategy is to encapsulate the Fe_3O_4 nanoparticles with carbon. The carbon coating could minimize the exposure between the Fe^0 nanograins and the organic electrolyte, as well as increase the electrical conductivity and accommodate volumetric expansion. Our Fe_3O_4@g-C nanorods, apparently, provide the right candidate to be investigated for reversible sodium storage. Figure 6a shows the typical voltage−time/capacity profiles for the first three cycles of sodium ion insertion−extraction in Fe_3O_4@g-C nanorods tested under a constant current. In the first cycle of sodium insertion, a storage capacity of 150 mAh/g was achieved. The first cycle irreversible capacity loss could be ascribed to the formation of solid electrolyte interphase (SEI) on the carbon surface. From the second cycle onward, the insertion−extraction profiles are highly similar, indicating the reversible electrochemical reactions involved. The cycle performance is shown in Figure 6b. However, the capacity is low as compared to the theoretical capacity.

Unfortunately, the low capacity may be ascribed to the graphite carbon coating. In contrast to lithium ions, sodium ions are significantly larger than lithium ions. Sodium ions cannot

significantly intercalate into graphitized carbon layers due to weak attractive interaction.[9,40−43] The carbon sheaths obtained under high temperature calcination with the presence of Fe_3O_4 are highly graphitized, as discussed above.[29,44] Therefore, the carbon sheaths act as shields that could prevent the sodium ions from having full access to the high-capacity Fe_3O_4 cores, leading to low unitization of cores in sodium ion storage. More direct evidence of the strong protection of the Fe_3O_4 cores that is provided by the carbon sheaths is found in the images collected from the electrodes after cycling (Figure 6c,d). As shown in the images, the rod-like morphology is well preserved and no significant volume expansion of the Fe_3O_4 cores was observed. The carbon sheaths expanded slightly due to the insertion of a small amount of sodium, but there were no notable changes in the cores.[43] It is known that volumetric expansion upon sodium pounding can easily break thin carbon shells and created asymmetric volumetric expansion of the cores.[45] Therefore, the graphite sheaths prevent the insertion of significant amounts of sodium ions into Fe_3O_4 cores, or do not allow the cores to participate meaningfully in the absorption of the sodium ions. Good stability was achieved, but at the sacrifice of specific capacity. It is known that disordered carbon can more easily take in sodium as compared to graphitic carbon.[9,41,46] This understanding actually provides indirect evidence that the carbon encapsulating the Fe_3O_4 is graphitic carbon. This analysis helps us to understand the low capacity observed. Therefore, it leads us to propose that future carbon sheaths should be focused on disordered carbon instead of graphitized carbon, regardless of the high capacity cores (such as Sn, Fe., Pb, Ge, Sn, P, metal oxides, alloys, or other high-capacity materials known to be electrochemically active toward sodium ions) for sodium-ion batteries in the future.[36,47−55] On the other hand, we also anticipate that there could be an optimal thickness for the carbon coating that would allow the sodium ions to access the Fe_3O_4 cores and maintain good stability even when the carbon is well graphitized. The thickness of the graphitized carbon coating should be less than 3 nm. Our ongoing effort is in those directions and results will be reported once available.

CONCLUSIONS

In summary, we developed a facile one-pot method for the preparation of amorphous carbon coated Fe_2O_3 nanorods that were easily converted to graphite carbon coated magnetic Fe_3O_4 nanorods. We demonstrated that the as prepared Fe_3O_4@g-C nanorods can reversibly adsorb a dye and be potentially used as recyclable adsorbents in the removal of toxins from water. At the same time, the magnetic Fe_3O_4@g-C nanorods are proposed to be employed as vehicles for the controlled release of drugs in an aqueous environment, particularly for use in targeted treatments through guided external magnetic forces. Additionally, Fe_3O_4@g-C nanorods were investigated for reversible absorption of sodium ions. We discovered that graphite carbon sheaths that encapsulate the high capacity Fe_3O_4 cores prevent the sodium ions from having full access to the cores. Although the absolute value of our Fe_3O_4@g-C nanorods in the reversible absorption of sodium ions is not high, the experimental results suggested that coating with graphitic carbon may not be suitable for electrode materials used in future sodium-ion batteries, in contrast to that of lithium-ion batteries. This important discovery is helpful in guiding future endeavors using carbon coating as a strategy to overcome pulverization in high-capacity candidates for sodium-ion batteries.

ASSOCIATED CONTENT

Supporting Information

EDS profiles of one-pot synthesized Fe_2O_3@C and the derived Fe_3O_4@C nanorods and FESEM images of samples. This material is available free of charge via the Internet at http://pubs.acs.org.

AUTHOR INFORMATION

Corresponding Author

*D. Deng. E-mail: da.deng@wayne.edu.

Notes

The authors declare no competing financial interest.

ACKNOWLEDGMENTS

The authors thank the Lumigen Instrument Center, Wayne State University, Detroit, MI.

REFERENCES

(1) Mahvi, A. H.; Ghanbarian, M.; Nasseri, S.; Khairi, A. Mineralization and discoloration of textile wastewater by TiO_2 nanoparticles. *Desalination* **2009**, *239*, 309−316.

(2) Li, J.; Zhou, Z. G.; Wang, H. J.; Li, G. F.; Wu, Y. Research on decoloration of dye wastewater by combination of pulsed discharge plasma and TiO_2 nanoparticles. *Desalination* **2007**, *212*, 123−128.

(3) Li, Y.-H.; Wang, S.; Wei, J.; Zhang, X.; Xu, C.; Luan, Z.; Wu, D.; Wei, B. Lead adsorption on carbon nanotubes. *Chem. Phys. Lett.* **2002**, *357*, 263−266.

(4) Li, Q.; Mahendra, S.; Lyon, D. Y.; Brunet, L.; Liga, M. V.; Li, D.; Alvarez, P. J. J. Antimicrobial nanomaterials for water disinfection and microbial control: Potential applications and implications. *Water Res.* **2008**, *42*, 4591−4602.

(5) Wang, B.; Wu, H.; Yu, L.; Xu, R.; Lim, T.-T.; Lou, X. W. Template-free formation of uniform urchin-like A-FeOOH hollow spheres with superior capability for water treatment. *Adv. Mater.* **2012**, *24*, 1111−1116.

(6) Lu, X. C.; Xia, G. G.; Lemmon, J. P.; Yang, Z. G. Advanced materials for sodium-beta alumina batteries: Status, challenges and perspectives. *J. Power Sources* **2010**, *195*, 2431−2442.

(7) Slater, M. D.; Kim, D.; Lee, E.; Johnson, C. S. Sodium-ion batteries. *Adv. Funct Mater.* **2013**, *23*, 947−958.

(8) Pan, H. L.; Hu, Y. S.; Chen, L. Q. Room-temperature stationary sodium-ion batteries for large-scale electric energy storage. *Energy Environ. Sci.* **2013**, *6*, 2338−2360.

(9) Palomares, V.; Serras, P.; Villaluenga, I.; Hueso, K. B.; Carretero-Gonzalez, J.; Rojo, T. Na-Ion batteries, Recent advances and present challenges to become low cost energy storage systems. *Energy Environ. Sci.* **2012**, *5*, 5884−5901.

(10) Kim, S. W.; Seo, D. H.; Ma, X. H.; Ceder, G.; Kang, K. Electrode materials for rechargeable sodium-ion batteries: Potential alternatives to current lithium-ion batteries. *Adv. Energy Mater.* **2012**, *2*, 710−721.

(11) Lu, Y.; Zhang, S.; Li, Y.; Xue, L. G.; Xu, G. J.; Zhang, X. W. Preparation and characterization of carbon-coated $NaVPO_4$f as cathode material for rechargeable sodium-ion batteries. *J. Power Sources* **2014**, *247*, 770−777.

(12) Ruffo, R.; Fathi, R.; Kim, D. J.; Jung, Y. H.; Mari, C. M.; Kim, D. K. Impedance analysis of $Na0.44MnO_2$ positive electrode for reversible sodium batteries in organic electrolyte. *Electrochim. Acta* **2013**, *108*, 575−582.

(13) Takachi, M.; Matsuda, T.; Moritomo, Y. Cobalt Hexacyanoferrate as Cathode Material for Na+ Secondary Battery. *Appl. Phys. Express* **2013**, *6*.

(14) D'Arienzo, M.; Ruffo, R.; Scotti, R.; Morazzoni, F.; Maria, C. M.; Polizzi, S. Layered $Na0.71CoO_2$: A powerful candidate for viable and high performance Na-batteries. *Phys. Chem. Chem. Phys.* **2012**, *14*, 5945−5952.

(15) Lu, Y. H.; Wang, L.; Cheng, J. G.; Goodenough, J. B. Prussian blue: A new framework of electrode materials for sodium batteries. *Chem. Commun.* **2012**, *48*, 6544−6546.
(16) Ellis, B. L.; Makahnouk, W. R. M.; Makimura, Y.; Toghill, K.; Nazar, L. F. A multifunctional 3.5 V iron-based phosphate cathode for rechargeable batteries. *Nat. Mater.* **2007**, *6*, 749−753.
(17) Oh, S.-M.; Myung, S.-T.; Yoon, C. S.; Lu, J.; Hassoun, J.; Scrosati, B.; Amine, K.; Sun, Y.-K. Advanced Na[Ni0.25Fe0.5Mn0.25]O_2/C-Fe_3O_4 sodium-ion batteries using EMS electrolyte for energy storage. *Nano Lett.* **2014**, *14*, 1620−1626.
(18) Komaba, S.; Mikumo, T.; Yabuuchi, N.; Ogata, A.; Yoshida, H.; Yamada, Y. Electrochemical insertion of Li and Na ions into nanocrystalline Fe_3O_4 and A-Fe_2O_3 for rechargeable batteries. *J. Electrochem. Soc.* **2010**, *157*, A60−A65.
(19) Wang, Y.; Zhang, L.; Gao, X.; Mao, L.; Hu, Y.; Lou, X. W. One-pot magnetic field induced formation of Fe_3O_4/C composite microrods with enhanced lithium storage capability. *Small* **2014**, *10*, 2815−2819.
(20) Chen, J. S.; Zhang, Y.; Lou, X. W. One-pot synthesis of uniform Fe_3O_4 nanospheres with carbon matrix support for improved lithium storage capabilities. *ACS Appl. Mater. Interfaces* **2011**, *3*, 3276−3279.
(21) Zhu, T.; Chen, J. S.; Lou, X. W. Glucose-assisted one-pot synthesis of FeOOH Nanorods and Their Transformation to Fe_3O_4@ carbon nanorods for application in lithium ion batteries. *J. Phys. Chem. C* **2011**, *115*, 9814−9820.
(22) Ozaki, M.; Kratohvil, S.; Matijević, E. Formation of monodispersed spindle-type hematite particles. *J. Colloid Interface Sci.* **1984**, *102*, 146−151.
(23) Deng, D.; Lee, J. Y. Hollow core-shell mesospheres of crystalline SnO_2 nanoparticle aggregates for high capacity Li^+ ion storage. *Chem. Mater.* **2008**, *20*, 1841−1846.
(24) Zhu, J.; Ng, K. Y. S.; Deng, D. Porous olive-like carbon decorated Fe_3O_4 based additive-free electrode for highly reversible lithium storage. *J. Mater. Chem. A* **2014**, *2*, 16008−16014.
(25) Deng, D.; Lee, J. Y. Direct fabrication of double-rough chestnut-like multifunctional Sn@C composites on copper foil: Lotus effect and lithium ion storage properties. *J. Mater. Chem.* **2010**, *20*, 8045−8049.
(26) Deng, D.; Lee, J. Y. Reversible storage of lithium in a rambutan-like tin-carbon electrode. *Angew. Chem., Int. Ed.* **2009**, *48*, 1660−1663.
(27) Lou, X. W.; Deng, D.; Lee, J. Y.; Archer, L. A. Preparation of SnO_2/carbon composite hollow spheres and their lithium storage properties. *Chem. Mater.* **2008**, *20*, 6562−6566.
(28) Yokokawa, C.; Hosokawa, K.; Takegami, Y. Low temperature catalytic graphitization of hard carbon. *Carbon* **1966**, *4*, 459−465.
(29) Liu, Y.; Ren, Z.; Wei, Y.; Jiang, B.; Feng, S.; Zhang, L.; Zhang, W.; Fu, H. Synthesis and applications of graphite carbon sphere with uniformly distributed magnetic Fe_3O_4 Nanoparticles (MGCSs) and MGCS@Ag, MGCS@TiO_2. *J. Mater. Chem.* **2010**, *20*, 4802−4808.
(30) Zhang, W. M.; Wu, X. L.; Hu, J. S.; Guo, Y. G.; Wan, L. J. Carbon coated Fe_3O_4 nanospindles as a superior anode material for lithium-ion batteries. *Adv. Funct. Mater.* **2008**, *18*, 3941−3946.
(31) Chin, K. C.; Chong, G. L.; Poh, C. K.; Van, L. H.; Sow, C. H.; Lin, J.; Wee, A. T. S. Large-scale synthesis of Fe_3O_4 nanosheets at low temperature. *J. Phys. Chem. C* **2007**, *111*, 9136−9141.
(32) Lin, C.-C.; Ho, J.-M. Structural analysis and catalytic activity of Fe_3O_4 nanoparticles prepared by a facile co-precipitation method in a rotating packed bed. *Ceram. Int.* **2014**, *40*, 10275−10282.
(33) Ai, L.; Zhang, C.; Chen, Z. Removal of methylene blue from aqueous solution by a solvothermal-synthesized graphene/magnetite composite. *J. Hazard. Mater.* **2011**, *192*, 1515−1524.
(34) Hameed, B. H.; Din, A. T. M.; Ahmad, A. L. Adsorption of methylene blue onto bamboo-based activated carbon: Kinetics and equilibrium studies. *J. Hazard. Mater.* **2007**, *141*, 819−825.
(35) Kang, X.-J.; Dai, Y.-L.; Ma, P.-A.; Yang, D.-M.; Li, C.-X.; Hou, Z.-Y.; Cheng, Z.-Y.; Lin, J. Poly(acrylic acid)-modified Fe_3O_4 microspheres for magnetic-targeted and pH-triggered anticancer drug delivery. *Chem.—Eur. J.* **2012**, *18*, 15676−15682.
(36) Hariharan, S.; Saravanan, K.; Ramar, V.; Balaya, P. A rationally designed dual role anode material for lithium-ion and sodium-ion batteries: Case study of eco-friendly Fe_3O_4. *Phys. Chem. Chem. Phys.* **2013**, *15*, 2945−2953.
(37) Yuan, S. M.; Li, J. X.; Yang, L. T.; Su, L. W.; Liu, L.; Zhou, Z. Preparation and lithium storage performances of mesoporous Fe_3O_4@C microcapsules. *ACS Appl. Mater. Interfaces* **2011**, *3*, 705−709.
(38) Chen, Y.; Xia, H.; Lu, L.; Xue, J. Synthesis of porous hollow Fe_3O_4 beads and their applications in lithium ion batteries. *J. Mater. Chem.* **2012**, *22*, 5006−5012.
(39) Xiong, Q. Q.; Tu, J. P.; Lu, Y.; Chen, J.; Yu, Y. X.; Qiao, Y. Q.; Wang, X. L.; Gu, C. D. Synthesis of hierarchical hollow-structured single-crystalline magnetite (Fe_3O_4) microspheres: The highly powerful storage versus lithium as an anode for lithium ion batteries. *J. Phys. Chem. C* **2012**, *116*, 6495−6502.
(40) Ge, P.; Fouletier, M. Electrochemical intercalation of sodium in graphite. *Solid State Ionics* **1988**, *28−30* (Part 2), 1172−1175.
(41) Slater, M. D.; Kim, D.; Lee, E.; Johnson, C. S. Sodium-ion batteries. *Adv. Funct. Mater.* **2012**, *23*, 947−958.
(42) Wenzel, S.; Hara, T.; Janek, J.; Adelhelm, P. Room-temperature sodium-ion batteries: Improving the rate capability of carbon anode materials by templating strategies. *Energy Environ. Sci.* **2011**, *4*, 3342−3345.
(43) Stevens, D. A.; Dahn, J. R. The mechanisms of lithium and sodium insertion in carbon materials. *J. Electrochem. Soc.* **2001**, *148*, A803−A811.
(44) Chen, Y.-J.; Xiao, G.; Wang, T.-S.; Ouyang, Q.-Y.; Qi, L.-H.; Ma, Y.; Gao, P.; Zhu, C.-L.; Cao, M.-S.; Jin, H.-B. Porous Fe_3O_4/carbon core/shell nanorods: Synthesis and electromagnetic properties. *J. Phys. Chem. C* **2011**, *115*, 13603−13608.
(45) Chen, W.; Deng, D. Sodium-cutting: A new top-down approach to cut open nanostructures on nonplanar surfaces on a large scale. *Chem. Commun.* **2014**, *50*, 13327−13330.
(46) Cao, Y. L.; Xiao, L. F.; Sushko, M. L.; Wang, W.; Schwenzer, B.; Xiao, J.; Nie, Z. M.; Saraf, L. V.; Yang, Z. G.; Liu, J. Sodium ion insertion in hollow carbon nanowires for battery applications. *Nano Lett.* **2012**, *12*, 3783−3787.
(47) Qian, J. F.; Wu, X. Y.; Cao, Y. L.; Ai, X. P.; Yang, H. X. High capacity and rate capability of amorphous phosphorus for sodium ion batteries. *Angew. Chem., Int. Edit* **2013**, *52*, 4633−4636.
(48) Kim, Y.; Park, Y.; Choi, A.; Choi, N. S.; Kim, J.; Lee, J.; Ryu, J. H.; Oh, S. M.; Lee, K. T. An amorphous red phosphorus/carbon composite as a promising anode material for sodium ion batteries. *Adv. Mater.* **2013**, *25*, 3045−3049.
(49) Bi, Z. H.; Paranthaman, M. P.; Menchhofer, P. A.; Dehoff, R. R.; Bridges, C. A.; Chi, M. F.; Guo, B. K.; Sun, X. G.; Dai, S. Self-organized amorphous TiO_2 nanotube arrays on porous Ti foam for rechargeable lithium and sodium ion batteries. *J. Power Sources* **2013**, *222*, 461−466.
(50) Zhu, H. L.; Jia, Z.; Chen, Y. C.; Weadock, N.; Wan, J. Y.; Vaaland, O.; Han, X. G.; Li, T.; Hu, L. B. Tin anode for sodium-ion batteries using natural wood fiber as a mechanical buffer and electrolyte reservoir. *Nano Lett.* **2013**, *13*, 3093−3100.
(51) Liu, Y. H.; Xu, Y. H.; Zhu, Y. J.; Culver, J. N.; Lundgren, C. A.; Xu, K.; Wang, C. S. Tin-coated viral nanoforests as sodium-ion battery anodes. *ACS Nano* **2013**, *7*, 3627−3634.
(52) Datta, M. K.; Epur, R.; Saha, P.; Kadakia, K.; Park, S. K.; Kuma, P. N. Tin and graphite based nanocomposites: Potential anode for sodium ion batteries. *J. Power Sources* **2013**, *225*, 316−322.
(53) Su, D. W.; Ahn, H. J.; Wang, G. X. Sno2@Graphene nanocomposites as anode materials for Na-ion batteries with superior electrochemical performance. *Chem. Commun.* **2013**, *49*, 3131−3133.
(54) Xu, Y. H.; Zhu, Y. J.; Liu, Y. H.; Wang, C. S. Electrochemical performance of porous carbon/tin composite anodes for sodium-ion and lithium-ion batteries. *Adv. Energy Mater.* **2013**, *3*, 128−133.
(55) Huang, J. P.; Yuan, D. D.; Zhang, H. Z.; Cao, Y. L.; Li, G. R.; Yang, H. X.; Gao, X. P. Electrochemical sodium storage of TiO_2(B) nanotubes for sodium ion batteries. *RSC Adv.* **2013**, *3*, 12593−12597.